Bull Earthquake Eng (2012) 10:1885–1909
DOI 10.1007/s10518-012-9381-8

ORIGINAL RESEARCH PAPER

Seismic fragility assessment of SMA-bar restrained multi-span continuous highway bridge isolated by different laminated rubber bearings in medium to strong seismic risk zones

M. Shahria Alam · M. A. Rahman Bhuiyan · A. H. M. Muntasir Billah

Received: 31 December 2011 / Accepted: 6 September 2012 / Published online: 22 September 2012

Abstract This study analytically determines the seismic fragility of a three-span continuous highway bridge fitted with laminated rubber bearings and shape memory alloy (SMA) restrainers. Fragility function, which expresses the likelihood of exceeding a damage state conditioned at a given earthquake intensity, has been derived based on SeismoStruct's nonlinear incremental dynamic analysis results of the bridge subjected to medium to strong earthquake excitation records. A total of 20 excitation records with peak ground acceleration values ranging from 0.45 to 1.07 g, are used in the nonlinear dynamic analysis of the bridge. A 2-D finite element model scheme is used in this study considering nonlinearity in the bridge piers and the isolation bearings. Two types of laminated rubber bearings are used in the bridge system in addition to the SMA restrainers: high damping rubber bearings and lead rubber bearings. The fragility curves are constructed for two bridge components (i.e. piers and isolation bearings), and the system as well. The component fragility curves are combined to evaluate the fragility curves for the entire bridge system at different damage states. The bridge system, for simplicity, considers the bridge deck, isolation bearings with SMA restrainer and bridge piers but excluding the bridge foundations and the abutments. The numerical results show that the failure probability of the bridge system is dominated by the bridge piers over the isolation bearings. Moreover, the inclusion of SMA restrainers in the bridge system exhibits high probability of failure, especially, when the system is isolated with lead rubber bearings.

Keywords Incremental dynamic analysis · Laminated rubber bearings · Shape memory alloy · Fragility function

1 Introduction

Highway bridges are one of the most common and critical components of a transportation network as they play important roles in evacuation and emergency routes for rescues, first-aid,

M. S. Alam (✉) · M. A. R. Bhuiyan · A. H. M. M. Billah
School of Engineering, University of British Columbia, Kelowna, BC, V1V1V7 Canada
e-mail: shahria.alam@ubc.ca

firefighting, medical services and transporting disaster commodities. However, they are very vulnerable to damages during major earthquakes (Basöz et al. 1999; Yamazaki et al. 2000). Past and recent earthquakes, such as the 1971 San Fernando earthquake, the 1994 Northridge earthquake, the 1995 Great Hanshin earthquake in Japan, and the 1999 Chi-Chi earthquake in Taiwan, the 2008 Sichuan earthquake, the 2010 Chile earthquake, the 2010 Haiti earthquake, the 2011 Christchurch earthquake have exposed the devastating nature of large earthquakes and its related economic impact.

In order to improve the seismic performance and subsequently reduce the seismic vulnerability of both new and retrofitted bridges, different forms of seismic isolation devices have been widely used for the last few decades (Buckle and Mayes 1990; Imbsen 2001; Naeim and Kelly 1996; Skinner et al. 1993). Due to the flexible property of isolation devices, the natural period of a bridge fitted with this kind of device can be increased in such way that the bridge resonance can be safely avoided. In addition, the inherently occupied damping property and energy dissipation mechanism prevents the bridge system from over-displacement (Kelly 1997). Field evidence on the seismic response of isolated bridges during recent earthquakes (Chaudhary et al. 2000, 2001), analytical studies (Diclel and Buddaram 2006; Ghobarah 1988; Ghobarah and Ali 1988; Karim and Yamazaki 2007; Ozbulut and Hurlebaus 2010, 2011; Wilde et al. 2000; Zhang and Huo 2009; Zhang et al. 2009) and experimental research (Kikuchi and Aiken 1997; Hwang et al. 2002) have revealed that the isolation devices can suppress the transmission of the input earthquake energy, and help improve the seismic performance of a bridge structure and subsequently reduce the cost for repair and rehabilitation after earthquakes.

Laminated rubber bearings and sliding bearings are the two major types of seismic isolation devices, which are usually adopted for highway bridges. The sliding bearings are introduced to separate, by providing frictional sliding, the transmitting earthquake induced forces from the input earthquakes. However, this system does not encompass any re-centering capability unless a friction pendulum sliding bearing is used. On the other hand, the laminated rubber bearings with high flexibility are meant to shift the natural period of bridges so as to avoid the resonance with excitations and they are usually occupied with damping properties to prevent the isolated bridges from excessive displacement. Due to its capability of supporting large loads while sustaining large movements with little or no maintenance requirement (Ali and Abdel-Ghaffar 1995), the laminated rubber bearings have been applied more frequently in highway bridges in recent years. Three types of laminated rubber bearings are widely used for this purpose: natural rubber bearing (NRB), lead rubber bearing (LRB), and high damping rubber bearing (HDRB). Out of these, HDRB and LRB, due to their high damping properties, are being widely used all over the world, especially in Japan and USA. However, laminated rubber bearings (HDRB and LRB) initiate some consequence -problems, such as (1) instability due to large deformation, and (2) un-recovered residual deformation, and (3) the necessity for replacement of the deformed bearings after a strong earthquake.

In order to overcome fully/partially the above mentioned limitations of the laminated rubber bearings, shape memory alloys (SMA) accompanied with laminated rubber bearings are reported to employ in the seismic isolation of highway bridge (Choi et al. 2005; DesRoches and Delemont 2002; Ozbulut and Hurlebaus 2010, 2011; Wilde et al. 2000). The superelasticity and hysteresis property of the SMA allows it to incorporate with laminated rubber bearings to reduce the residual deformation of the bridge system. SMA is a special kind of material with the ability to undergo large inelastic deformation but potentially fully recover its strain by heating (shape memory effect) or by unloading (superelasticity). SMA, due to its inherited restoring and energy dissipation capacity, is getting wide research interest in seismic

protection of highway bridges, e.g. Choi et al. (2005), Ozbulut and Hurlebaus (2011) etc. In their studies, they showed that the isolation bearing consisting of laminated rubber bearings and SMA is capable of supplying enough damping with the inherent re-centering ability and subsequently restricting the relative displacement of the bridge deck. Moreover, the effectiveness of using the SMA in the isolation system in improving the seismic performance of the bridge system has been demonstrated in the past studies. Wilde et al. (2000) also carried out the seismic performance assessment of a bridge pier, isolated with elastomeric bearings and SMA bars being attached below the bridge deck and top of the pier, subjected to earthquake ground motions in transverse direction. The isolation system was verified as an effective device to control relative deck displacement. DesRoches and Delemont (2002) conducted numerical analysis of a multiple span simply supported bridge, isolated with elastomeric bearings and SMA restrainers, subjected to earthquake ground motions in longitudinal direction. They showed that the SMA bars are more effective to restrain relative deck displacement than the conventional steel cable restrainers. However, a recent study by Bhuiyan and Alam (2012) shows that the seismic vulnerability increases with the use of SMA restrainers in an isolated bridge. They conducted seismic fragility assessment on SMA-restrained multi-span continuous highway bridge isolated by laminated rubber bearings under low to medium seismic ground motion. The have considered two seismic response parameters, namely displacement ductility of piers and shear displacement of laminated rubber bearings. In their study, they have concluded that the bridge pier is more vulnerable than the laminated rubber bearing with an increasing trend of vulnerability in case of SMA-restrained bridge. However, the use of SMA might be advantageous under medium to large earthquake ground motions where it will be subjected to higher strain to utilize its superelastic behavior. Therefore, further study is required in this direction.

Vulnerability assessment of bridges is a widely recognized useful approach for prioritization of seismic retrofitting decisions, disaster response planning, estimation of direct monetary loss, and evaluation of loss of functionality of highway systems in the event of an earthquake. Seismic vulnerability of highway bridges is usually expressed in the form of fragility curves, which display the conditional probability where the structural demand (structural response) caused by various levels of ground shaking exceeds the structural capacity defined by a damage state. Bridge vulnerability information is useful in assessing, managing, and reducing seismic risk. There are different fragility-curve generation methodologies involving probabilistic seismic performance evaluation of highway bridges. Some of these methodologies are based on expert opinion (ATC 1985) whereas some are based on empirically formulated equations on observed damages from past earthquakes (Basöz and Kiremidjian 1998; Shinozuka et al. 2000a,b; Yamazaki et al. 2000), while others are derived from analytical simulation methods (Bignell and LaFave 2009; Choi et al. 2004; Hwang et al. 2000, 2001; Karim and Yamazaki 2001, 2007; Mackie and Stojadinović 2004, 2007; Nielson 2005; Nielson and DesRoches 2007a,b; Padgett and DesRoches 2008; Bhuiyan and Alam 2012). Though all of the methodologies have their own limitations in evaluating the probabilistic seismic performance of highway bridges, fragility assessment methodologies using analytical approaches have become widely adopted since they are more readily applicable to bridge types and geographical regions where seismic bridge damage records are insufficient.

The objective of this work is to assess the vulnerability of a three-span continuous highway bridge isolated by laminated rubber bearings and SMA restrainers when subjected to medium to strong earthquakes. Here, analytical simulation based method is used to evaluate the seismic fragility of the bridge, which is based on the results obtained from nonlinear incremental dynamic analysis (IDA) using a finite element (FE) package SeismoStruct (2011). In this study high damping rubber bearings (HDRB) and lead rubber bearings (LRB) are utilized

for seismic isolation, in addition to SMA restrainer as a supplementary device to provide energy dissipation and re-centering capability. A 2-D finite element model scheme with nonlinear force-displacement relationships for the bridge piers and the isolation bearings are used in the analytical modeling of the bridge. Nonlinear incremental dynamic analysis of the isolated bridge are then performed for a total of 20 earthquake excitations of peak ground acceleration (PGA) magnitudes ranging from 0.45 to 1.07 g. The seismic responses of the bridge components (piers and isolation bearings) are utilized to evaluate the likelihood of exceeding the seismic capacity of each component. Then the individual component fragility functions derived from the IDA results are combined to evaluate the overall fragility of the bridge system.

2 Methodology of seismic fragility function

This study employs probabilistic seismic demand model (PSDM) to derive the analytical fragility curves using nonlinear time-history analysis of the bridge system. The PSDM establishes a correlation between the engineering demand parameters (EDP) and the ground intensity measures (IM). In the current study, ductility of the bridge pier and horizontal deformation of the isolation bearing are considered as the EDPs, and the PGA is utilized as the intensity measure (IM) of each ground motion record. Two approaches are used to develop the PSDM: the scaling approach (Zhang and Huo 2009) and the cloud approach (Choi et al. 2004; Mackie and Stojadinović 2004; Nielson and DesRoches 2007a,b). In the scaling approach, all the ground motions are scaled to selective intensity levels and an incremental dynamic analysis (IDA) is conducted at each level of intensity; whereas in the cloud approach, un-scaled earthquake ground motions are used in the nonlinear time-history analysis and then a probabilistic seismic demand model is developed based on the nonlinear time history analysis results. In the current study, only the IDA method is utilized in evaluating the seismic fragility functions of the bridge components and system as well. In the IDA each increment involves a full nonlinear time history analysis of the bridge structure to capture its behavior under that particular ground motion intensity. IDA is carried out by scaling each ground motions to ten intervals and generating 200 data sets for the regression analysis of demand for a given IM. For carrying out the IDA the ground motions are not scaled to a particular intensity rather they are scaled from a very low PGA to a maximum PGA of 2.0 g. This helped in reducing the computational time but provided adequate damage data for generating fragility curves. Each intensity level of a particular ground motion can be considered as one time history analysis. Thus it was possible to generate sufficient damage data corresponding to different intensity levels. In this approach, no priori assumption is required for probabilistic distribution of seismic demand in order to derive the fragility curves. The occurrence ratio at a specified damage state (DS) is computed and directly used as the damage probability at the given IM level, i.e. the damage probability is calculated as the ratio of the number of damage cases n_i for the damage state i over the number of total simulation cases N:

$$P\left[EDP > DS_i \,|IM|\right] = \frac{n_i}{N} \tag{1}$$

The fragility curves as derived using IDA approach can be expressed in most cases using a lognormal cumulative distribution function:

$$P\left[EDP > DS_i \,|IM|\right] = \int_{-\infty}^{IM} \frac{1}{IM\sqrt{2\pi\xi_{IM}^2}} \exp\left[-\frac{[\ln(IM) - \lambda]^2}{2\xi_{IM}^2}\right] d(IM), \tag{2a}$$

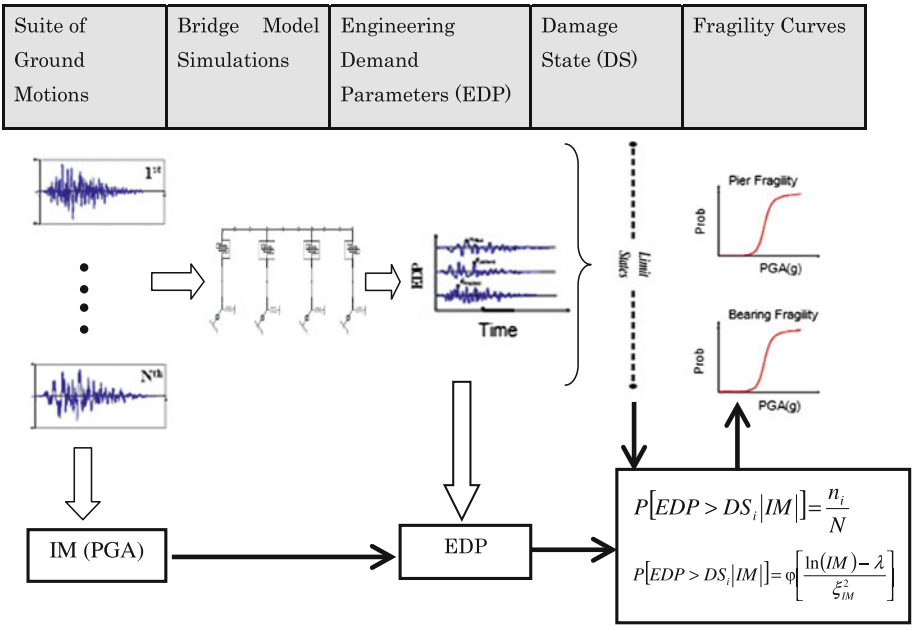

Fig. 1 A flow chart describing the generation methodology of fragility curve

Equation 2 can be equivalently re-written in a very usual form as

$$P\left[EDP > DS_i\,|IM|\right] = \varphi\left[\frac{\ln\left(IM\right) - \lambda}{\xi_{IM}^2}\right] \tag{2b}$$

where φ is the normal distribution, and λ and ξ^2 are, respectively, mean and standard deviation of IMs based on lognormal distribution. Figure 1 depicts a flow chart that describes the methodology for generating fragility curves from the bridge component responses.

For bridges under earthquake induced forces, bridge components experience different damage states causing a comprehensive damage state of the bridge system, which cannot be expressed by only one component's damage state and therefore, fragility function of the bridge system is more convincing than the component level fragility function (Choi et al. 2004; Mackie and Stojadinović 2007; Nielson and DesRoches 2007a,b; Zhang and Huo 2009). The first order reliability theory can be used to derive the upper and lower bounds on the system fragility function. This theory is only valid for a series type system where failure of one component causes failure of the entire system. When the bridge is modeled in longitudinal direction as in the current study, it in fact behaves like a series system as presented in Figs. 2 and 3. Following the first order reliability theory the global damage state of the system can be evaluated by considering the largest damage state at component level as follows

$$DS_{system} = \max\left(DS_{pier}, DS_{bearing}\right) \tag{3}$$

The lower bound of the system fragility gives un-conservative estimate of the failure probability of the system, whereas the upper bound indicates the conservative estimate of the failure probability of the system which can be mathematically expressed as

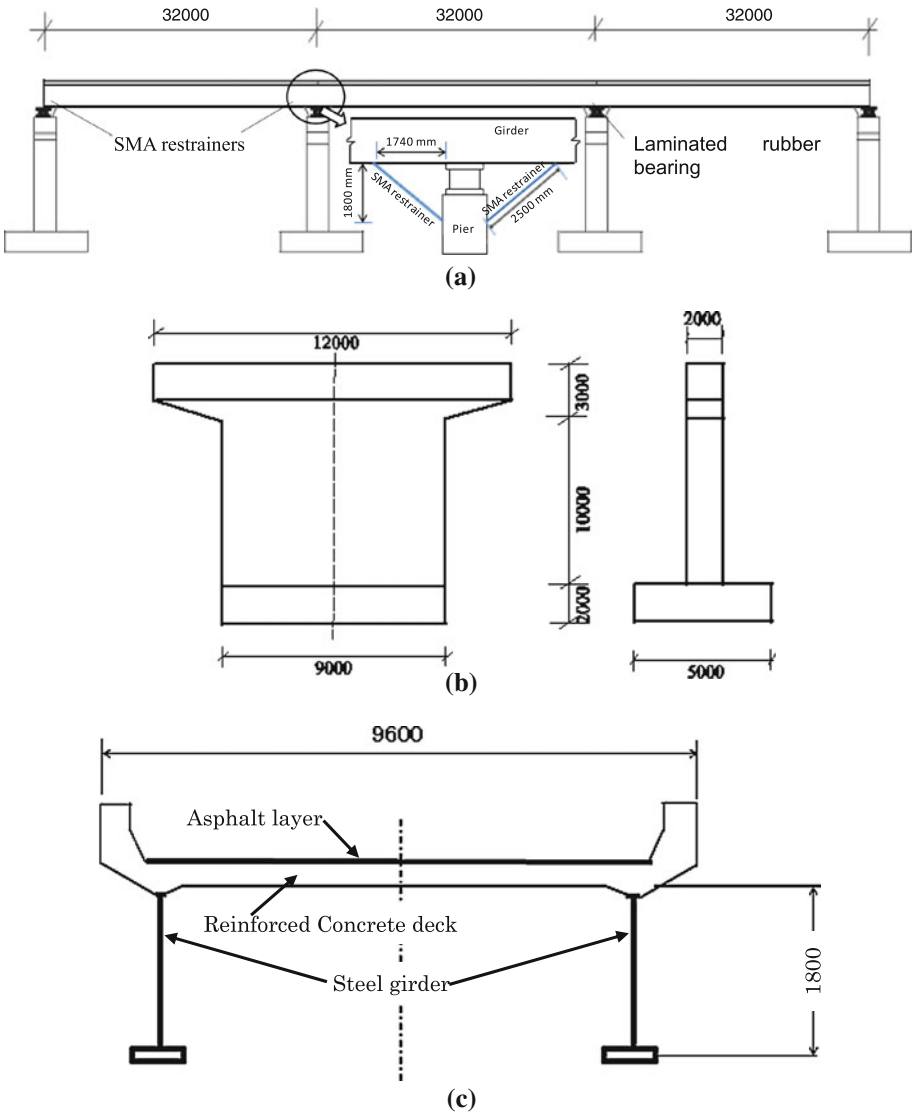

Fig. 2 Geometric details of the bridge **a** longitudinal view of the bridge, and **b** transverse and longitudinal view of the bridge pier, **c** transverse section of the superstructure; all dimensions are in mm

$$\max_{i=1}^{n}[P(F_i)] \leq P\left(F_{system}\right) \leq 1 - \prod_{i=1}^{n}[1 - P(F_i)], \tag{4}$$

where $P(F_i)$ and $P\left(F_{system}\right)$ is the likelihood of reaching the prescribed limit of damage state of the component and system, respectively. Another possibility of estimating the system fragility functions could be using the joint probabilistic seismic demand model (JPSDM) and capacity model of the bridge components (Nielson 2005; Nielson and DesRoches 2007a); however, in the current study the former one (Eq. 4) has been strategically utilized to evaluate the seismic fragility of the bridge system.

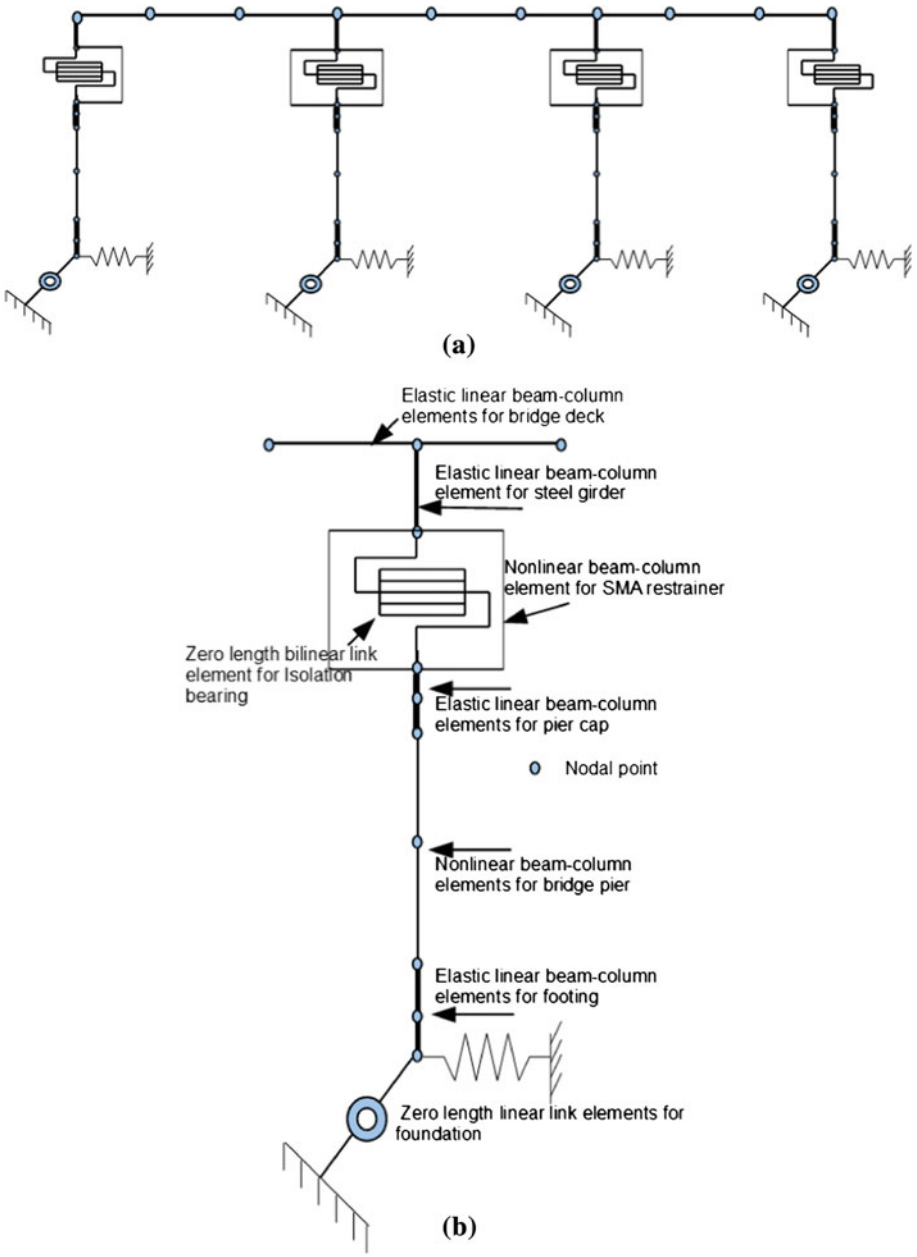

Fig. 3 Analytical model of the bridge system **a** 2-D finite element model of the bridge system including nonlinear model used for isolation bearings and bridge pier, and **b** details of modeling of an internal bridge pier

3 Characterization of damage states

For seismically isolated highway bridges with continuous composite deck-girder system, bridge piers and isolation bearings are the most critical components, which are often forced

Table 1 Damage/limit state of bridge components

Damage state	→	Slight (DS = 1)	Moderate (DS = 2)	Extensive (DS = 3)	Collapse (DS = 4)	References
Bridge components	Physical phenomenon	Cracking and spalling	Moderate cracking and spalling	Degradation without collapse	Failure leading to collapse	FEMA (2003)
Bridge pier	Displacement ductility μ_d	$\mu_d > 1.0$	$\mu_d > 1.2$	$\mu_d > 1.76$	$\mu_d > 4.76$	Hwang et al. (2001)
Isolation bearing	Shear strain $\gamma(\%)$	$\gamma > 100$	$\gamma > 150$	$\gamma > 200$	$\gamma > 250$	Zhang and Huo (2009)

to enter into nonlinear range of deformations under strong earthquakes. Different forms of EDPs, ductility of bridge piers, and horizontal deformation of isolation bearings are used to measure the damage state (DS) of the bridge components. A capacity model is needed to measure the damage of bridge component based on prescriptive and descriptive damage states in terms of EDPs (FEMA 2003; Choi et al. 2004; Nielson 2005). Four damage states as defined by HAZUS (FEMA 2003) are commonly adopted in the seismic vulnerability assessment of engineering structures, namely slight, moderate, extensive and collapse damages. Table 1 summarizes the definitions of various damage states and their corresponding damage criteria available in the literature.

The damage states of isolation devices are determined based on experimental observation as well as consideration of resulting pounding and unseating. Typically either the bearing displacement or shear strain is used to describe the damage states, as shown in Table 1. Previous studies (Abe et al. 2004; Bhuiyan 2009) show that the mechanical behavior of laminated rubber bearings portrays three distinct features such as initial high stiffness at very low strain levels, almost constant stiffness at low to moderate strain levels due to its Payne's effect and finally high stiffness at high strain levels (e.g. 150 %) due to its strain hardening effects. Moreover, strain-rate and temperature induced viscosity property is observed in the bearings, especially in high damping rubber bearings (Bhuiyan et al. 2009; Bhuiyan 2009). Although the modern isolation bearings can experience shear strain up to 400 % before failure, such large shear strain will result in large displacement and can cause significant pounding or unseating problem in the bridge system. Therefore, once the shear strain exceeds 250 %, it is considered as complete damage of the bearing (JRA 2002). In this study, the shear strain for isolation bearings and the displacement ductility for the bridge pier are adopted as damage index (DI) to capture the damage states.

4 Structural properties of the bridge

A typical three-span continuous highway bridge, isolated by laminated rubber bearings and restrained with SMA bars, is used in the current study as shown in Fig. 2. The bridge consists of continuous reinforced concrete (RC) deck-steel girder (as shown in Fig. 2c) isolated by laminated rubber bearings installed below the steel girder supported on RC piers (Fig. 2a). In addition, two SMA bars are used at each bridge pier being attached between the top of bridge pier and bottom of the girder (Fig. 2a).

Table 2 Geometries and material properties of the bridge

Properties	Specifications
Cross-section area of the pier cap (mm^2)	$2,000 \times 12,000$
Cross-section area of the pier body (mm^2)	$2,000 \times 9,000$
Cross-section area of the footing (mm^2)	$5,000 \times 9,000$
Height of the pier (mm)	15,000
Young's modulus of elasticity of concrete (N/mm^2)	25,000
Young's modulus of elasticity of steel (N/mm^2)	200,000

Table 3 Geometries and materials properties of the isolation bearings and Ni-Ti SMA

Dimension	Specifications	
	HDRB	LRB
Cross-section of the bearing (mm^2)	600×600	600×600
Thickness of rubber layers (mm)	81	75
Number of rubber layers	6	6
Thickness of steel layer (mm)	3.0	3.0
Nominal shear modulus (MPa)	1.2	1.2
Number of lead plugs	–	4
Diameter of lead plugs (mm)	–	90
Cross-section of SMA restrainer bar (mm^2)	1,256	
Length of SMA restrainer bar (mm)	2,500	

The superstructure consists of 260 mm RC slab covered by 80 mm of asphalt layer. The height of the continuous steel girder is 1,800 mm. The substructures consist of RC piers and footings supported on shallow foundation (Fig. 2b). The reinforcement details of the bridge pier consist of D29 (diameter 29 mm) longitudinal reinforcements along the longer direction being distributed @ 200 mm c/c except at the corners where the spacing of the reinforcements is 125 mm c/c and D29 (diameter 29 mm) reinforcements along the shorter direction being distributed @ 200 mm c/c except at the corners where the spacing is limited to 150 mm c/c. The hoop reinforcement in both directions are D22 (diameter 22 mm) being distributed @ 125 mm c/c. The dimensions and material properties of the bridge deck, piers with footings are given in Table 2. The geometry and material properties of laminated rubber bearings and SMA are presented in Table 3.

5 Analytical modeling of the bridge

As the current study considers a longitudinally straight multi-span continuous highway bridge, the entire system is approximated as a continuous 2-D finite element frame using the SeismoStruct nonlinear analysis program (SeismoStruct 2011).The analytical model of the bridge system is shown in Fig. 3a. The 2-D model approach has been proven sufficient for numerical analysis when the bridge is longitudinally straight. In this regard, the works of Choi et al. (2004, 2005), DesRoches and Delemont (2002), Zhang and Huo (2009) can be referred. For instance, Zhang and Huo (2009) derived fragility curves of a longitudinally straight base isolated highway bridge using both 2D and 3D finite element models and concluded that the two models of the bridge have almost identical results. Although the current analysis has been performed using a freely available software, the authors have verified the

software with several experimental results that consist of static and dynamic loading of structures. For instance, static pushover test of an RC bridge bent by Billah (2011), shake table test of an SMA RC column by Alam et al. (2008), quasi-static reversed cyclic loading test of an SMA RC beam-column joint by Alam et al. (2008) and Billah and Alam (2012), and shake table test of a three storey RC frame by Alam et al. (2009). Besides, the software SeismoStruct was employed by the winner in the Practitioners category at the recent blind prediction contest deployed by PEER and NEES with the shake-table testing of a full-scale circular bridge pier (NEES-PEER 2011).

A finite element model with frame and spring elements is used to approximate the continuous system of the bridge with a finite number of degrees of freedom. The superstructure and substructure of the bridge are modeled as a lumped mass system divided into a number of small discrete segments. The mass of each segment is assumed to be distributed between the two adjacent nodes in the form of point mass. The details of modeling of a typical bridge pier along with deck are given in Fig. 3b.

5.1 Modeling of concrete deck, steel girders, pier caps and footing

The superstructure consisting of RC bridge deck and steel girders is modeled using linear beam-column elements so that the superstructure remains elastic under the seismic loads applied in the longitudinal direction. It should be noted that the stiffness of the superstructure does not have a significant effect on the seismic response of the bridge (Ghobarah and Ali 1988) since the longitudinal response is typically governed by the isolation bearings, bridge piers, and foundation (Choi et al. 2004). The bridge piers are modeled using the fiber elements. Each fiber has a stress–strain relationship, which can be specified to represent unconfined concrete, confined concrete, and longitudinal steel reinforcement. The confinement effect of the concrete section is considered on the basis of reinforcement detailing as discussed in the preceding section. The distribution of inelastic deformation and forces is sampled by specifying cross-section slices along the length of the element. The nonlinear force-displacement behavior of the bridge pier should be considered in seismic analysis of a bridge system, especially in a seismically active zone. In such a region, the bridge piers are expected to incur large displacements during earthquakes, which lead to the fact that the linear force-displacement behavior of a bridge pier will result in a very uneconomic design. As the current work considers medium to strong earthquake ground motion records, the nonlinear force displacement behavior of the bridge piers have been selected. The pier footings are modeled using linear elastic elements. The footing-foundation movement is modeled using two linear translational and rotational springs. The medium ground condition is used in the analysis. The characteristic value (T_G) of the ground ranges from 0.2 to 0.6 s (JRA 2002).

5.2 Modeling of laminated rubber bearings

HDRBs and LRBs, due to their high damping properties, are being widely used all over the world. HDRBs possess various mechanical properties, which are influenced by their compounding effect (Hwang et al. 2002), nonlinear elasto-plastic behavior (Abe et al. 2004; Bhuiyan 2009) and temperature and strain-rate dependent viscosity property (Bhuiyan 2009; Bhuiyan et al. 2009; Dall'Asta and Ragni 2006). LRBs also acquire all the mechanical properties of HDRBs with reduced extent (Bhuiyan 2009; Robinson 1982).

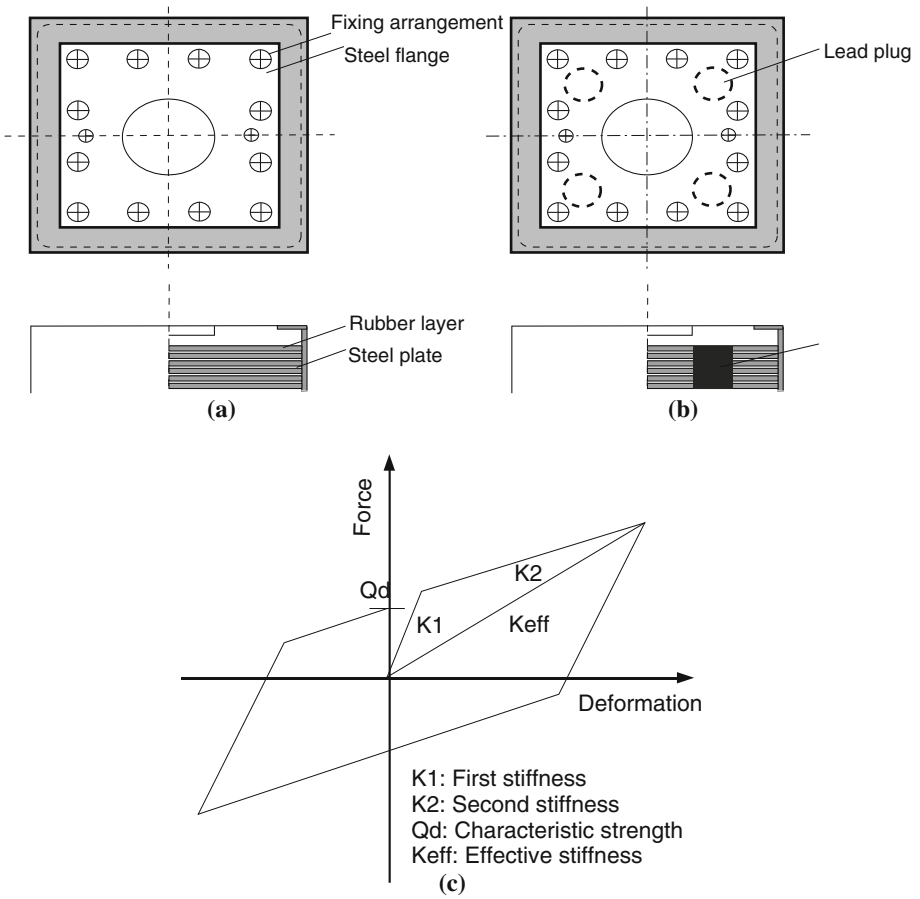

Fig. 4 **a** Typical arrangement of HDRB, **b** typical arrangement of LRB, and **c** bilinear model of laminated rubber bearing as used in AASHTO (2000) and JRA (2002)

Two types of laminated rubber bearings are used in this study, namely high damping rubber bearings (HDRB) and lead rubber bearings (LRB). The mechanical behavior of laminated rubber bearings, especially HDRBs, are mainly dominated by strain magnitude (Abe et al. 2004; Bhuiyan et al. 2009), strain-rate (Bhuiyan et al. 2009; Dall'Asta and Ragni 2006) and also compounding effect (Hwang et al. 2002) etc.

Moreover, the mechanical behavior of laminated rubber bearings can be characterized by three distinct features: a high initial stiffness at very small strain levels, an almost constant stiffness at small to medium strain levels followed by a high stiffness due to its inherently occupied strain hardening features. So, a constitutive model capable of replicating the strain-rate and the strain level dependent mechanical behavior of laminated rubber bearing is required for simulating the mechanical responses when subjected to earthquake induced ground motions. However, for brevity, the current study considers the design bilinear model (Fig. 4) as proposed in code specifications (AASHTO 2000; JRA 2002). The model parameters of the bearings are estimated as per the recommendations from JRA (2002) as presented in Table 4.

Table 4 Design parameters of isolation bearings: HDRB and LRB

	HDRB	LRB
Elastic stiffness, K1, (kN/m)	36,000	30,000
Post yield stiffness, K2, (kN/m)	4,173	4,221
Characteristic strength, Qd (kN)	212	200
Effective stiffness, Keff (kN/m)	5,791	5,840
Effective damping ratio (%)	16.9	16.7

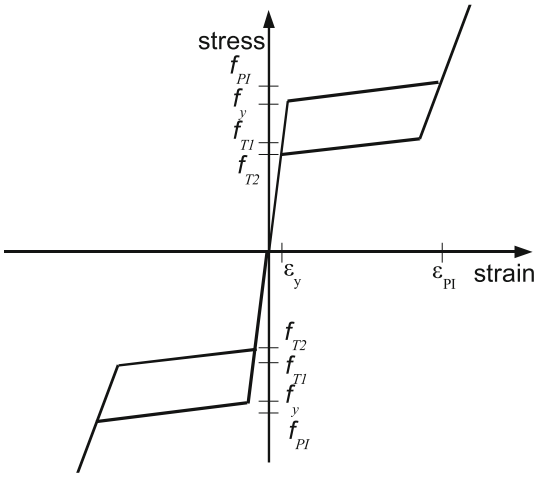

Fig. 5 A typical one-dimensional superelastic model of shape memory alloy with its characteristic stress and strain

5.3 Modeling of shape memory alloy

In general, the constitutive model of SMA is very complicated in a sense that it depends upon many factors, such as strain rates, strain magnitude and strain history (Wei et al. 2002). Three categories of constitutive models are used for characterizing the superelasticity and damping properties of SMA, such as parametric, nonparametric and differential equation-based models. However, the differential equation-based constitutive model (Auricchio et al. 1997; Auricchio and Sacco 1997; Wei et al. 2002) is widely used for SMA since it is capable of using in continuum mechanics based FE algorithms considering small and finite deformations and subsequently in finite element based professional software packages, such as ANSYS (2010) and SeismoStruct (2011) etc.

The 1-D constitutive model for SMA as proposed by Auricchio and Sacco (1997) and Auricchio et al. (1997) is adopted in this work. This model is capable of reproducing both superelasticity and damping properties of SMA. The premise of this model is to consider SMA as a composite material comprising of austenite and martensite, which allows evaluating the modulus of elasticity of the composite material in terms of modulus of elasticity of each component (austenite and martensite) and an internal state variable known as martensite fraction, which is evaluated using some evolution equations. A typical stress–strain relationship of SMA is schematically illustrated in Fig. 5. Several parameters are used to express the complete stress–strain relationship of SMA. Table 5 presents the required parameters for Ni-Ti based SMA model used in the present analysis. Figure 6 shows the stress–strain curves of the SMA model (Auricchio et al. 1997) with a complete transformation path followed by (a) cycles with partial loading (PL) and partial unloading (PU), (b) cycles with PL and complete

Table 5 Constitutive parameters of Ni-Ti based SMA

Parameters	Unit	Value
Austenite to martensite starting stress, f_y	MPa	410
Austenite to martensite finishing stress, f_{P1}	MPa	470
Martensite to austenite starting stress, f_{T1}	MPa	170
Martensite to austenite finishing stress, f_{T2}	MPa	140
Yield strain limit, ε_y	%	1
Recoverable pseudoelastic strain limit, ε_{Pl}	%	7

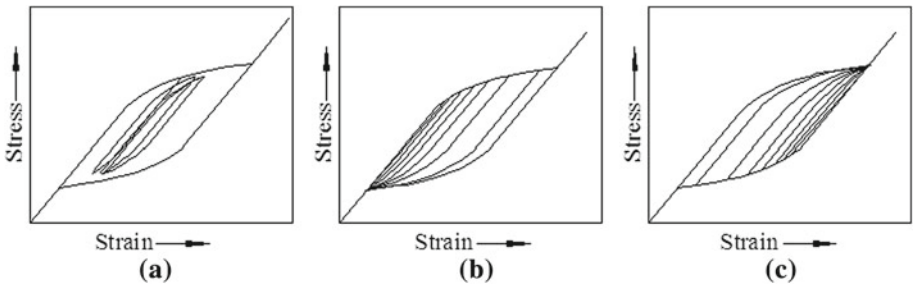

Fig. 6 1D-Superelastic model of SMA at constant temperature where the stress–strain curves are drawn after a complete transformation path followed by **a** PL and PU, **b** PL and CU, and **c** CL and PU (reprinted from Auricchio et al. (1997) with permission)

unloading (CU), and (c) cycles with complete loading (CL) and PU, respectively. Here, PL and PU refer to incomplete stress induced phase transformation, whereas CL and CU refer to complete stress induced transformation in the loading-unloading process, respectively.

6 Seismic ground motion records

A data set comprising inputs (ground motion records) and outputs (damage) is necessary to establish a relationship between earthquake ground motion and structural damage. In this regard, two methods are usually employed: collect the actual earthquake records and damage data, and perform earthquake response analysis for given inputs and models and subsequently obtain the resultant damages. Though the former one is more realistic and convincing, it is very difficult and sometimes impossible to get adequate earthquake records near structural damage. The latter is relatively easy to construct well-distributed data comprising input ground motions and structural damage since it is not based on actual seismic damage records. Nevertheless, much care has to be taken while selecting models of the structure and input ground motions. The nonlinear time history analysis take the nonlinearity of the members into account, and responses of the bridge are subsequently dependent on the characteristics of earthquake ground motions. So, the uncertainty characteristics of the earthquake ground motions regarding ground type, intensity and frequency contents have a great effect on nonlinear time history responses of members. Moreover, it is important to properly select input motion parameters to correlate with structural damage.

The PGA is a widely used index to describe the severity of the earthquake ground motion (Mackie and Stojadinović 2007; Padgett and DesRoches 2008). However, it is recognized that a large value of PGA is not always followed by severe structural damages. Other indices of earthquake ground motion, e.g., peak ground velocity (PGV)

Table 6 Characteristics of the earthquake ground motion histories

SL no	Earthquake	Year	Richter magnitude	PGA (g)	PGV (cm/s)
1	Tabas	1978	7.4	0.922	108.0
2	Tabas	1978	7.4	0.958	103.8
3	Loma Prieta	1989	7.0	0.703	170.0
4	Loma Prieta	1989	7.0	0.458	89.3
5	Loma Prieta	1989	7.0	0.672	175.0
6	Duzce, Turkey	1999	7.1	0.728	56.44
7	Mendocino	1992	7.1	0.625	123.4
8	Mendocino	1992	7.1	0.651	91.0
9	Erzincan	1992	6.7	0.448	57.0
10	Landers	1992	7.3	0.691	133.4
11	Landers	1992	7.3	0.793	69.0
12	Nothridge	1994	6.7	0.872	171.0
13	Nothridge	1994	6.7	0.721	120.0
14	Nothridge	1994	6.7	0.583	52.9
15	Kobe	1995	6.9	1.071	157.0
16	Kobe	1995	6.9	0.563	71.0
17	Kobe	1995	6.9	0.774	170.5
18	Kobe	1995	6.9	0.686	156.7
19	Kobe	1995	6.9	0.673	129.6
20	Kobe	1995	6.9	0.736	108.4

(Nielson 2005), peak ground displacement (PGD), time duration of strong motion (Td), spectrum intensity (SI) and spectral characteristics can also be considered in damage assessment.

A suite of 20 earthquake ground motion records (Table 6), which are assigned as medium to strong magnitude earthquake ground motions (JRA 2002) with PGA values ranging from 0.45 to 1.07 g have been considered in the current study. The characteristics of the earthquake ground motion records are presented in Table 6. Figure 7a shows the acceleration response spectra with 5 % damping ratio of the recorded ground motions. The mean amplitude of the earthquake records is also accompanied in the figure. Figure 7b shows the different percentiles of acceleration response spectra with 5 % damping ratio illustrating that the selected earthquake ground motion records are well describing the medium to strong intensity earthquake motion histories as per the Japanese Code (JRA 2002).

7 Numerical results and discussion

In order to assess the seismic vulnerability of a three-span continuous highway bridge, seismic fragility curves for the piers and isolation bearings are generated using the numerical results obtained from the nonlinear incremental dynamic analysis. The bridge is isolated with two types of laminated rubber bearings along with SMA restrainers. Assuming a lognormal distribution with respect to the median of seismic intensity (PGA), the fragility curves for two bridge components: pier and isolation bearing are generated using Eqs. (1) and (2) and calibrating with the capacity limit states as shown in Table 1. In this regard, a number of incremental dynamic analysis of the bridge subjected to longitudinal excitations using 20 ground motion records of PGA magnitudes ranging from 0.45 to 1.07 g are carried out. Each

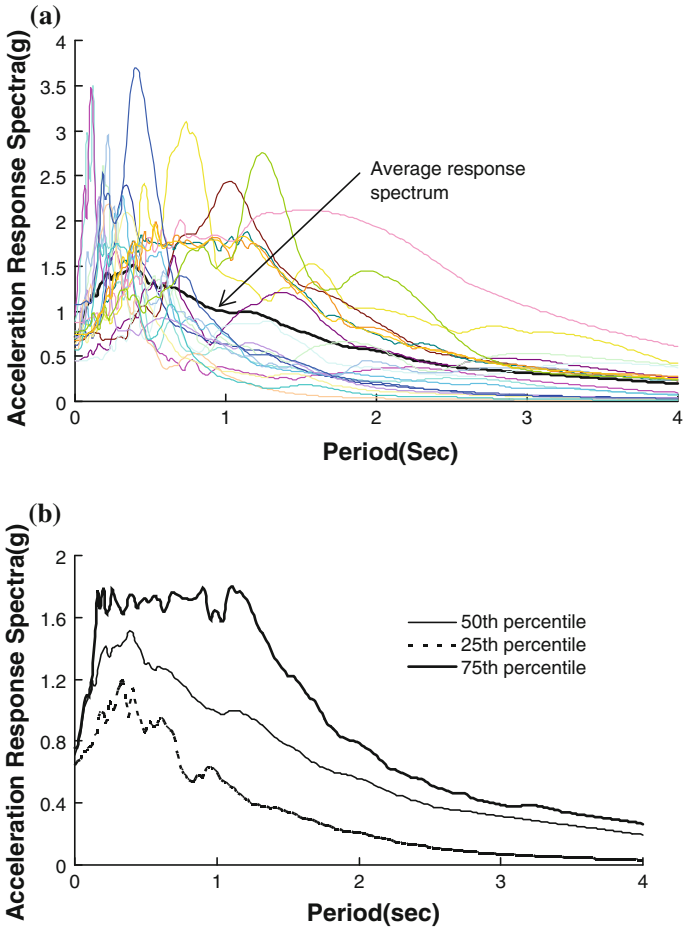

Fig. 7 Earthquake ground motion records, **a** response acceleration spectra, **b** percentiles of response acceleration spectra of a suit of 20 near field earthquake ground motion records. The values PGAs range from 0.45 to 1.07 g

ground motion record is scaled at different intensity levels up to 2.0 g PGA, which is then used in the incremental dynamic analysis. Nonlinear model for bridge piers, isolation bearings and SMA are considered in this analysis. Moreover, the Rayleigh damping approach is employed in order to estimate the damping of the bridge.

7.1 Fragility of bridge piers

Figures 8 and 9 present the fragility curves of the bridge piers isolated by high damping and lead rubber bearings. Figure 8a, b present the fragility curves for the bridge pier isolated by HDRB without and with SMA restrainers, respectively. The most vulnerable pier is considered in deriving the fragility curves for different damage states (DS) as recommended by HAZUS-MH (FEMA 2003), such as slight, medium, extensive and collapse. As can be observed from Fig. 8a, b, the inclusion of SMA device in the isolation system significantly

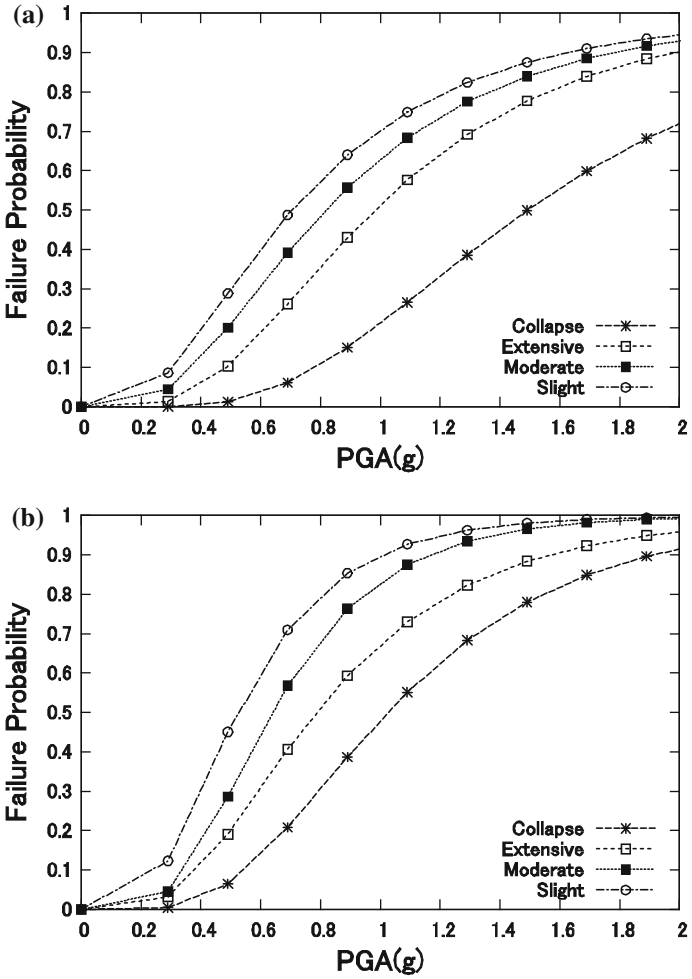

Fig. 8 Fragility curves of the bridge pier isolated with high damping rubber bearings **a** without SMA restrainers and **b** with SMA restrainers

increases the seismic vulnerability of the bridge pier in all damage states at each earthquake intensity level. This can be attributed that the inclusion of SMA device induces an additional stiffness to the bridge system causing a higher seismic force demand being attracted to the bridge pier (Wilde et al. 2000).

From Fig. 8b it can be observed that the inclusion of SMA restrainer in the isolation system causes a little increase in the seismic fragility of the bridge pier for a given damage state. The bridge pier restrained with SMA bars increases the bearings forces, which results in an increased pier displacement leading to comparatively higher seismic vulnerability. The fragility curves of the bridge pier isolated by LRB with and without SMA restrainers as presented in Fig. 9a, b, respectively were similar to those of the HDRBs.

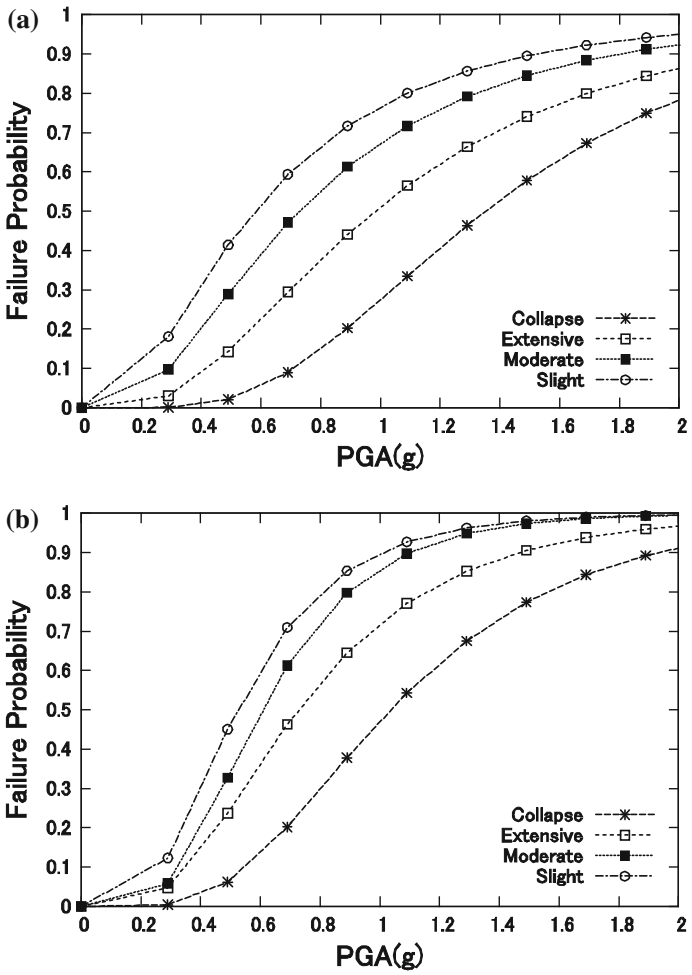

Fig. 9 Fragility curves of the bridge pier isolated with lead rubber bearings **a** without SMA restrainers **b** with SMA restrainers

7.2 Fragility of isolation bearings

Figures 10 and 11 present the fragility of isolation bearings used in the bridge system. Figure 10a, b display the fragility curves for the HDRB without and with SMA restrainers, respectively. A total of four isolation bearings are used in the bridge to accommodate the vertical and lateral deformations as experienced, respectively from the vertical compressive loadings of the bridge deck and the earthquake ground motions. Only the most vulnerable bearing is utilized to derive the fragility curves. From each figure it is revealed that the inclusion of SMA restrainer in the isolation system causes a little increase in the seismic fragility of the HDRB for the given damage states, which further induces the seismic vulnerability of the bearing and the bridge deck. Similar trends are observed in the fragility curves for LRB systems as presented in Fig. 11a, b.

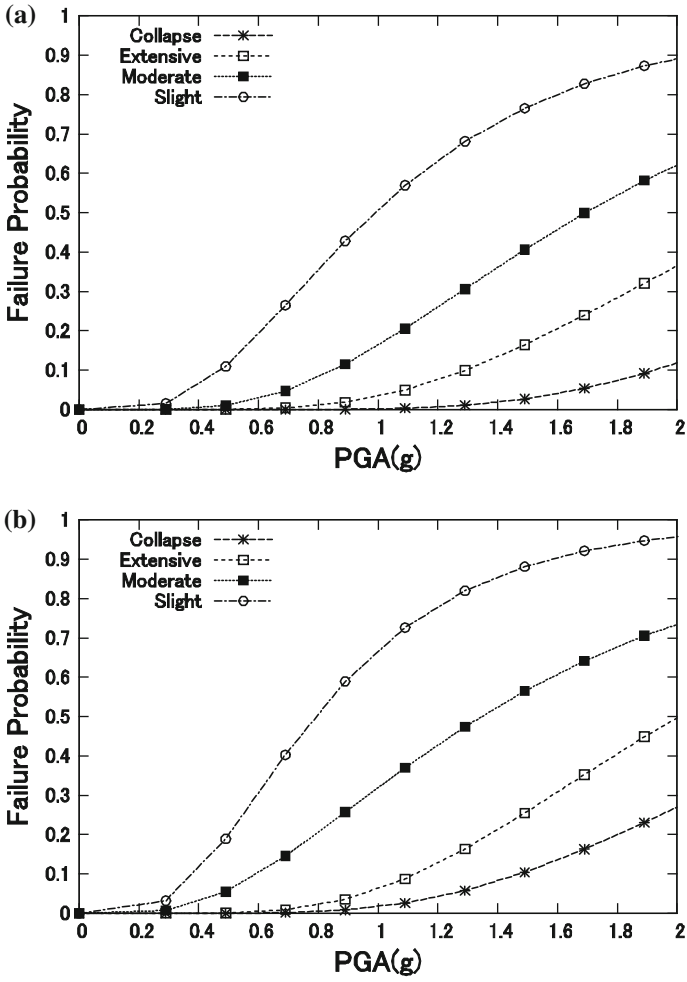

Fig. 10 Fragility curves of high damping rubber bearings **a** without SMA restrainers and **b** with SMA restrainers

The numerical results as depicted in Figs. 8, 9, 10, 11 illustrate the relative likelihood of reaching/exceeding certain damage state conditioned at a given seismic intensity level for bridge components (pier and isolation bearing), which indicates that the bridge piers possess more seismic vulnerability than the isolation bearings (HDRB/LRB). Consequently, bridge piers should be given higher preference over the isolation bearings in designing new bridges, and prioritization of retrofitting strategies of old bridges.

7.3 Fragility of bridge system

The fragility curves of a bridge system can be subsequently constructed by combining the fragility curves as obtained for each bridge component (pier and isolation bearing). This can be performed through a crude Monte Carlo simulation; however, it is computationally more expensive than the current simulations done in this work. Using the first order reliability

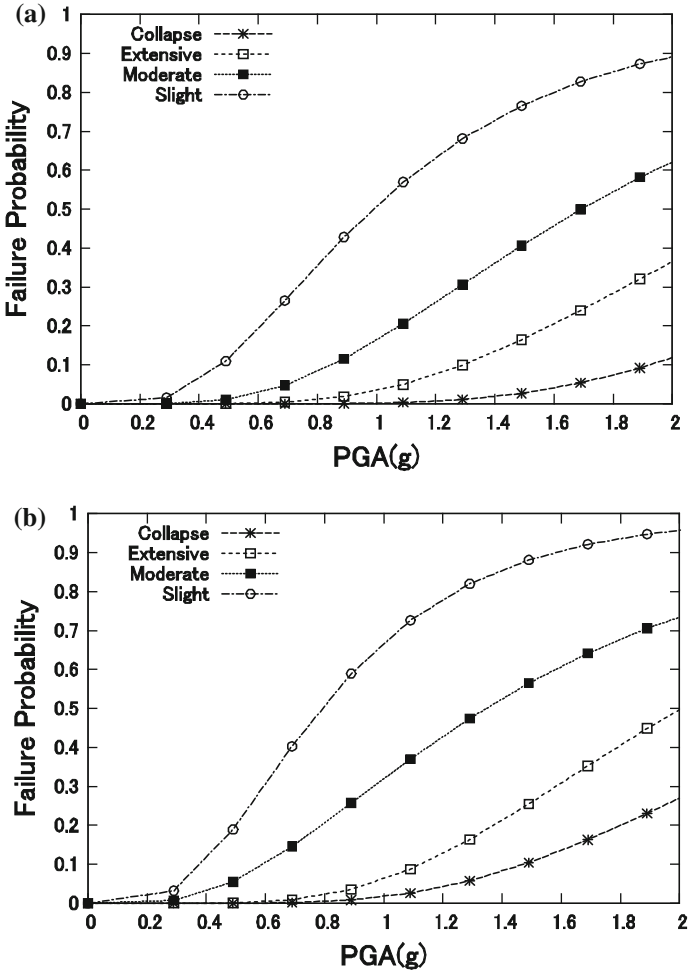

Fig. 11 Fragility curves of lead rubber bearings **a** without SMA restrainers and **b** with SMA restrainers

theory (Eq. 4), the fragility curves for the bridge system are generated for each damage state. Since the difference between the upper and lower bounds of the system fragility is not significant, the upper bounds of the fragility curves are presented in Figs. 12 and 13. Assuming a lognormal distribution, two lognormal distribution parameters λ and ξ^2 for the bridge system, the mean and standard deviation of the logarithmic intensity measures (IMs), are evaluated using a standard regression analysis method. The values of the two parameters are presented in Table 7.

Figure 12a, b present the fragility curves for the bridge system isolated by HDRB without and with SMA restrainers, respectively. In each figure, the four damage states are displayed to illustrate the seismic fragility of the bridge system. While comparing between the two figures, it can be observed that the seismic fragility of the bridge system slightly increases at each damage state with the inclusion of SMA restrainers. A similar trend with very little different magnitudes is also observed in the case of a bridge system isolated by LRB without and with SMA restrainers as shown in Fig. 13a, b, respectively. The numerical results

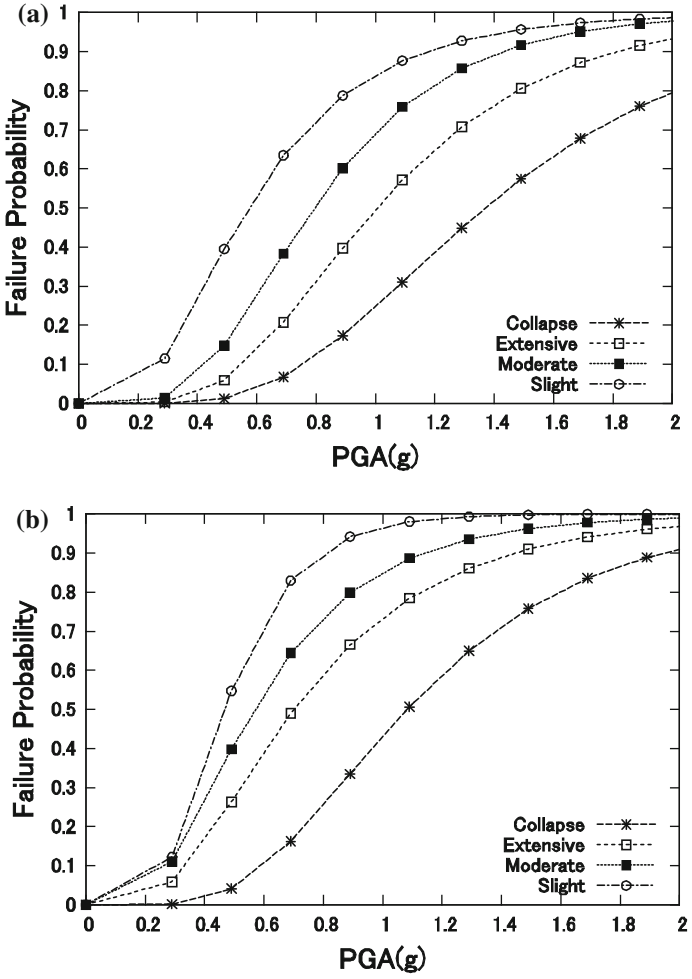

Fig. 12 Fragility curves of the bridge system isolated with high damping rubber bearings **a** without SMA restrainers and **b** with SMA restrainers

obtained for the bridge system isolated by HDRB and LRB are comparable to each other. The results illustrated in the two figures indicate that the seismic fragility of the bridge system is largely dictated by the fragility of bridge piers. Similar trends are also observed in the fragility curves at component levels.

7.4 Comparison of median values of PGA

Finally, the median of the probability of exceedance is determined for the bridge system with/without SMA restrainers at each damage level. Figure 14a shows a plot of the PGAs for the median values of probability of damage of the bridge system isolated by HDRB. From this figure it can be observed that the bridge system with SMA restrainers portrays seismically more fragile condition than that without SMA restrainers at each damage state. Similar trend

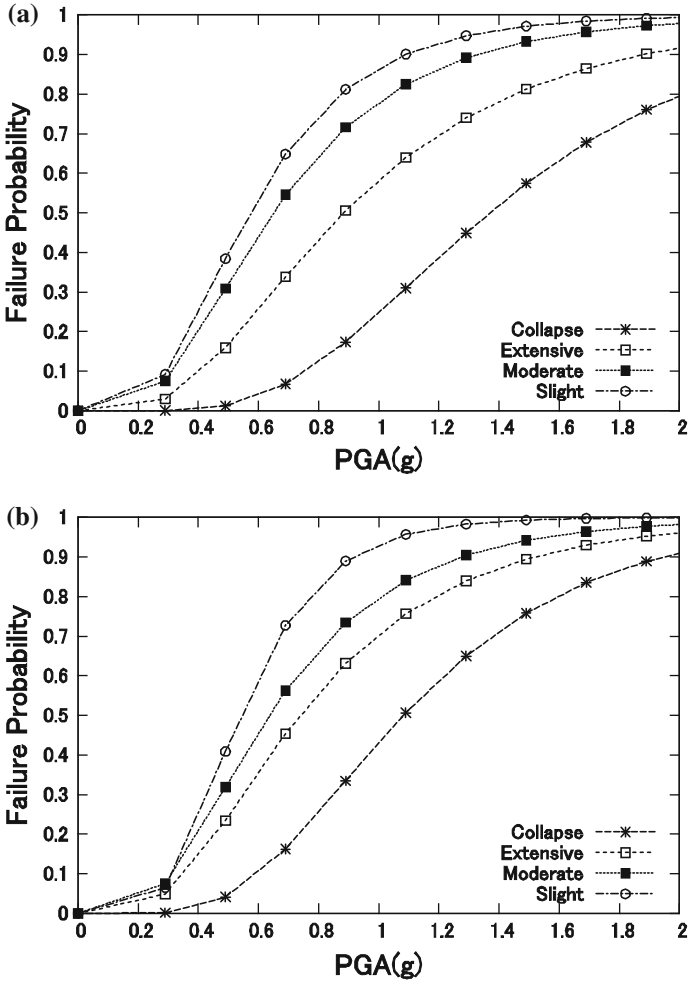

Fig. 13 Fragility curves of the bridge system isolated with lead rubber bearings **a** without SMA restrainers and **b** with SMA restrainers

Table 7 Parameters of fragility curves for the bridge system with respect to PGA

Damage state		Slight		Moderate		Extensive		Collapse	
Type of isolation		λ	ξ^2	λ	ξ^2	λ	ξ^2	λ	ξ^2
HDRB	With SMA	−0.76	0.41	−0.57	0.54	−0.35	0.56	0.08	0.46
	Without SMA	−0.56	0.57	−0.24	0.46	0.05	0.46	0.31	0.46
LRB	With SMA	−0.62	0.41	−0.46	0.56	−0.31	0.56	0.08	0.46
	Without SMA	−0.56	0.51	−0.44	0.56	−0.12	0.59	0.43	0.46

is also observed in the bridge system isolated by LRB with comparatively smaller median values of probability of damage as presented in Fig. 14b, which indicates that the bridge system isolation with LRB is seismically more vulnerable than that isolated with HDRB.

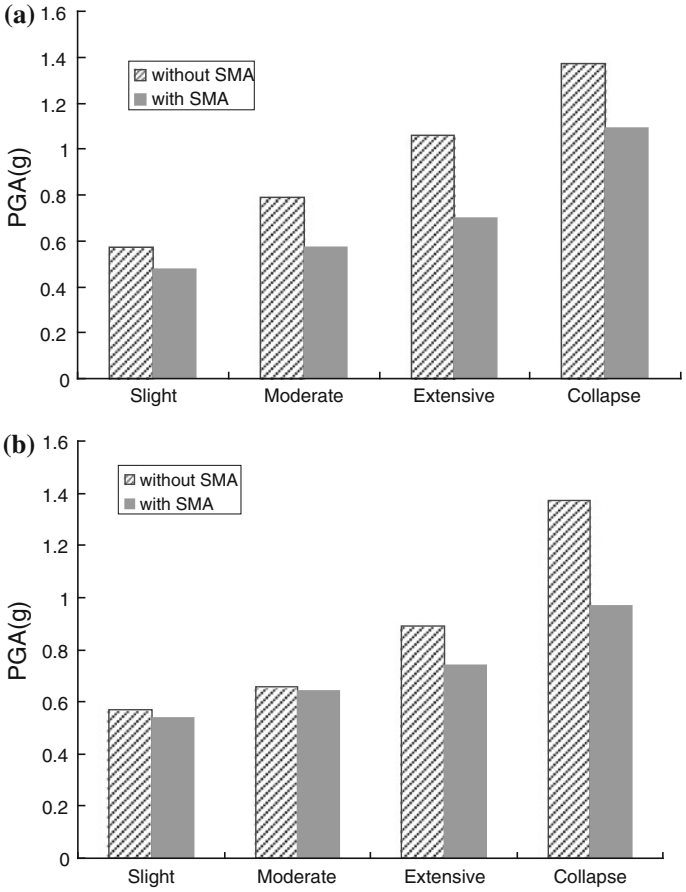

Fig. 14 Comparison of median values of PGA for the bridge system with/without SMA restrainers used in the isolation system, such as **a** high damping rubber bearing and **b** lead rubber bearing

8 Concluding remarks

This study presents the development of fragility curves of a three-span continuous highway bridge fitted with SMA restrainer and laminated rubber bearings. The fragility curves are generated analytically by modeling the bridge in the longitudinal direction. These curves obtained from this study can be potentially used to estimate the probable losses incurred from earthquakes, retrofitting prioritization and post-earthquake rehabilitation decision making. Based on the analysis the following conclusions can be drawn:

- The numerical results show that the bridge piers are more susceptible to damage for the given medium to strong seismic ground motions as compared to those of the isolation bearings.
- The seismic fragility of the bridge pier and the system increases with the inclusion of the SMA restrainers in the isolation system.
- The bridge system isolated with LRB experiences more seismic vulnerability than that isolated with HDRB when displacement ductility is considered as the demand parameter.

- The numerical results, based upon the median values of the PGA for the various damage states, show that the median PGA for the bridge system with SMA bars are comparatively lower than the bridge system without SMA bars, for each of the damage states.

Since the present study considers only one bridge model without considering uncertainty in geometry and material parameters, further study using various bridge models with different sets of geometry/ material properties should be conducted for better understanding the contributions of other parameters on the seismic fragility of a bridge system. Moreover, other intensity measures of the ground motions and SMA restrainers with different mechanical properties should also be considered while constructing the analytical fragility curves of the bridge system. These curves may be improved as more information is collected on the individual responses of the various bridge components in both transverse and longitudinal directions. Future study should include the effect of abutments and the foundations on the fragility responses.

Acknowledgments The first author gratefully acknowledges the financial contribution of Natural Sciences and Engineering Research Council (NSERC) of Canada for conducting this research.

References

Abe M, Yoshida J, Fujino Y (2004) Multiaxial behaviors of laminated rubber bearings and their modeling I: experimental study. J Struct Eng ASCE 130:1119–1132

Alam MS, Youssef MA, Nehdi M (2008) Analytical prediction of the seismic behavior of superelastic shape memory alloy reinforced concrete elements. Eng Struct 30(12):3399–3411

Alam MS, Youssef MA, Nehdi M (2009) Seismic performance of concrete frame structures reinforced with superelastic shape memory alloys. Smart Struct Syst 5(5):565–585

Ali HM, Abdel-Ghaffar AM (1995) Modeling of rubber and lead passive-control bearings for seismic analysis. J Struct Eng ASCE 121:1134–1144

AASHTO (2000) Guide specification for seismic isolation design, 2nd edn. American Association of State Highways and Transportation Officials, Washington DC, USA

ANSYS Inc (2010) ANSYS version 12.0. ANSYS, Inc

Applied Technology Council (ATC) (1985) Earthquake damage evaluation data for California. Report No. ATC-13

Auricchio F, Sacco E (1997) A superelastic shape-memory-alloy beam model. J Intell Mater Syst Struct 8:489–501

Auricchio F, Taylor RL, Lubliner J (1997) Shape-memory alloys: macromodelling and numerical simulations of the superelastic behavior. Comput Methods Appl Mech Eng 146:281–312

Basöz N, Kiremidjian AS (1998) Evaluation of bridge damage data from the Loma Prieta and Northridge. California Earthquakes Technical Report MCEER-98-0004, Multidisciplinary Center for Earthquake Engineering Research, State University of New York at Buffalo, Buffalo, NY

Basöz N, Kiremidjian AS, King SA, Law KH (1999) Statistical analysis of bridge damage data from the 1994 Northridge, CA, earthquake. Earthq Spectra 15(1):25–54

Bhuiyan M AR, Alam MS (2012) Seismic vulnerability assessment of a multi-span continuous highway bridge fitted with shape memory alloy bar and laminated rubber bearing. Earthq Spectra 28(4).

Bhuiyan AR, Okui Y, Mitamura H, Imai T (2009) A rheology model of high damping rubber bearings for seismic analysis: identification of nonlinear viscosity. Int J Solids Struct 46:1778–1792

Bhuiyan AR (2009) Rheology modeling of laminated rubber bearings, PhD dissertation. Graduate School of Science and Engineering, Saitama University, Japan

Bignell J, LaFave J (2009) Analytical fragility analysis of southern Illinois wall pier supported bridge pier. Earthq Eng Struct Dyn 39:709–729

Billah AHMM (2011) Seismic performance evaluation of multi-column bridge bent retrofitted with different alternatives. Master's thesis, 2011. School of Engineering, the University of British Columbia, Kelowna, Canada

Billah AHMM, Alam MS (2012) Seismic performance of concrete columns reinforced with hybrid shape memory alloy and fibre reinforced polymer bars. Constr Build Mater 28(3):730–742

Buckle IG, Mayes RL (1990) Seismic isolation: history, application, and performance—a world view. Earthq Spectra 6:161–201
Chaudhary MTA, Abe M, Fujino Y (2001) Performance evaluation of base-isolated Yama-agé bridge with high damping rubber bearings using recorded seismic data. Eng Struct 23:902–910
Chaudhary MTA, Abe M, Fujino Y, Yoshida J (2000) System identification of two base-isolated bridges using seismic records. J Struct Eng ASCE 126:1187–1195
Choi E, DesRoches R, Nielson BG (2004) Seismic fragility of typical bridges in moderate seismic zones. Eng Struct 26:187–199
Choi E, Nam TH, Cho BS (2005) A new concept of isolation bearings for highway steel bridges using shape memory alloys. Can J Civil Eng 32:957–967
Dall'Asta A, Ragni L (2006) Experimental tests and analytical model of high damping rubber dissipating devices. Eng Struct 28:1874–1884
DesRoches R, Delemont M (2002) Seismic retrofit of simply supported bridges using shape memory alloys. Eng Struct 24:325–332
Diclel M, Buddaram S (2006) Effect of isolator and ground motion characteristics on the performance of seismic-isolated bridges. Earthq Eng Struct Dyn 35:233–250
Federal Emergency Management Agency (FEMA) (2003) HAZUS-MH software, Washington DC
Ghobarah A, Ali HM (1988) Seismic performance of highway bridges. Eng Struct 10:157–166
Ghobarah A (1988) Seismic behavior of highway bridges with base isolation. Can J Civil Eng 15:72–78
Hwang H, Jernigan JB, Lin YW (2000) Evaluation of seismic damage to memphis bridges and highway systems. J Bridge Eng ASCE 5:322–330
Hwang H, Liu JB, Chiu YH (2001) Seismic fragility analysis of highway bridges. MAEC report: project MAEC RR-4. Mid-America Earthquake Center, Urbana
Hwang JS, Wu JD, Pan T, Yang G (2002) A mathematical hysteretic model for elastomeric isolation bearings. Earthq Eng Struct Dyn 31:771–789
Imbsen RA (2001) Use of isolation for seismic retrofitting bridges. J Bridge Eng ASCE 6:425–438
JRA (2002) Specifications for highway bridges-part V: seismic design. Japan Road Association, Tokyo, Japan
Karim KR, Yamazaki F (2007) Effect of isolation on fragility curves of highway bridges based on simplified approach. Soil Dyn Earthq Eng 27:414–426
Karim KR, Yamazaki F (2001) Effect of earthquake ground motions on fragility curves of highway bridge piers based on numerical simulation. Earthq Eng Struct Dyn 30:1839–1856
Kelly JM (1997) Earthquake resistant design with rubber. 2. Springer, Berlin
Kikuchi M, Aiken ID (1997) An analytical hysteresis model for elastomeric seismic isolation bearings. Earthq Eng Struct Dyn 26:215–231
Mackie KR, Stojadinović B (2004) Fragility curves for reinforced concrete highway overpass bridges. 13th WCEE, ID 1553
Mackie KR, Stojadinović B (2007) Performance-based seismic bridge design for damage and loss limits states. Earthq Eng Struct Dyn 36:1953–1971
Naeim F, Kelly J (1996) Design of seismic isolated structures. 1. Wiley, New York
NEES-PEER (2011) Concrete column blind prediction contest 2010. Accessed on Sept 2011; available at http://nisee2.berkeley.edu/peer/prediction_contest
Nielson BG (2005) Analytical fragility curves for highway bridges in moderate seismic zones, Ph.D. thesis, Georgia Institute of Technology, Atlanta
Nielson BG, DesRoches R (2007) Seismic fragility curves for typical highway bridge classes in the central and southeastern United States. Earthq Spectra 23:615–633
Nielson BG, DesRoches R (2007) Seismic fragility methodology for highway bridges using a component level approach. Earthq Eng Struct Dyn 36:823–839
Ozbulut OE, Hurlebaus S (2010) Evaluation of the performance of a sliding-type base isolation system with a NiTi shape memory alloy device considering temperature effects. Eng Struct 32:238–249
Ozbulut OE, Hurlebaus S (2011) Seismic assessment of bridge structures isolated by a shape memory alloy/rubber-based isolation system. Smart Mater Struct 20:015003
Padgett JE, DesRoches R (2008) Methodology for the development of analytical fragility curves for retrofitted bridges. Earthq Eng Struct Dyn 37:157–174
Robinson WH (1982) Lead rubber hysteresis bearings suitable for protecting structures during earthquakes. Earthq Eng Struct Dyn 10:593–604
SeismoStruct (2011) SeismoStruct help file. Available from www.seismsoft.com
Shinozuka M, Feng MQ, Kim HK, Kim SH (2000) Nonlinear static procedure for fragility curve development. J Eng Mech ASCE 126:1287–1295
Shinozuka M, Feng MQ, Lee J, Naganuma T (2000) Statistical analysis of fragility curves. J Eng Mech ASCE 126:1224–1231

Skinner RI, Robinson WH, McVerry GH (1993) An introduction to seismic isolation. DSIR Physical Science, Wellington

Wei Z, MA H, Sun D (2002) A mathematical model for pseudoelasticity of shape memory alloy and its application in passive control. J Vib Control 8:41–49

Wilde K, Gardoni P, Fujino Y (2000) Base isolation system with shape memory alloy device for elevated highway bridges. Eng Struct 22:222–229

Yamazaki F, Motomura H, Hamada T (2000) Damage assessment of expressway networks in Japan based on seismic monitoring. 12th WCEE, ID 0551

Zhang Y, Hu X, Zhu S (2009) Seismic performance of benchmark base-isolated bridges with superelastic Cu-Al-Be restraining damping device. Struct Control Health Monit 16:668–685

Zhang J, Huo Y (2009) Evaluating effectiveness and optimum design of isolation devices for highway bridges using the fragility function method. Eng Struct 31:1648–1660